DYNAMIC TARGETING FOR IMPROVED TRACKING OF STORM FEATURES

Alberto Candela, Jason Swope, Steve Chien, Hui Su, and Peyman Tavallali

Jet Propulsion Laboratory
California Institute of Technology
4800 Oak Grove Dr, Pasadena, CA 91109, USA

ABSTRACT

Dynamic Targeting (DT) will enable future Earth Observing instruments to intelligently reconfigure and point instruments to dramatically enhance science return. In this work we present a realistic simulation study of DT for tracking of storm features. To this end we have developed several algorithms from Operations Research and Artificial Intelligence/heuristic search. We benchmark these algorithms and show that DT is a powerful tool with the potential to significantly improve science yield.

Index Terms— dynamic targeting, artificial intelligence, storm science.

1. INTRODUCTION

While a new generation of unprecedented miniaturized Earth observing instruments has emerged, fundamental physics of remote sensing dictates that high spatial resolution at reduced size (and therefore power, cost) forces reduced swath. This places a premium on measurement on acquiring the highest science value data enabled by pointable instruments.

Dynamic targeting (DT) can improve the efficiency of conventional expensive narrow swath instruments. DT uses information from a lookahead sensor to identify targets for the primary sensor which can then be pointed or reconfigured to improve science yield. DT also addresses a major inefficiency in many Earth observing missions, where the majority of their data is not usable due to cloud cover and other poor observing conditions. Additionally, for other instruments that may be limited by energy, data volume, or configuration, DT can be used to best operate an instrument by turning on only when high value targets are detected (to conserve energy), varying compression/summarization (to conserve data volume), and control other instrument settings (gain, frequency, chirp rate, etc.). DT is applicable across a wide range of missions and will enable far better coverage of transient phenomena, such as storm systems that are of high scientific interest. We expect it to become commonplace across many if not most future Earth Science missions.

In this work we present a simulation study focused on using DT for effectively tracking rare storm features. To this end we have developed several algorithms that draw from a rich heritage of methods including Operations Research, as well as Artificial Intelligence/heuristic search methods. We benchmark these algorithms and show that DT is a powerful tool for improving science return.

2. RELATED WORK

Rapid cloud screening has been used onboard aircraft to remove and compress clouds to reduce data volume [1]. Another example of cloud avoidance work has been completed on TANSO-FTS-2 where intelligent targeting is utilized to minimize observations compromised by the presence of clouds [2]. Hasnain et al. at NASA Jet Propulsion Laboratory use both a greedy and a graph search based algorithm to select the most clear sections of sky during a flyover [3]. Similar ongoing work includes the Smart Ice Cloud Sensing (SMICES) smallsat concept, a radar application that intelligently targets storms and clouds [4]. Despite the opposite goal of the cloud-minimization problem, it operates in a similar manner by picking an area in the instrument field of view to analyze. SMICES targets images at a rapid rate, on the order of seconds, and its planner runs as a continuous problem. Moreover, SMICES uses multiple cloud labels to identify different targets instead of the labels used for cloud avoidance (cloud vs. clear). This gives SMICES flexibility on which targets to analyze and allows scientists to tailor its algorithm to target the clouds that best align with their scientific interests.

3. SIMULATION STUDY

The simulation study consists of an Earth science satellite whose mission is to analyze storm clouds. The satellite has two onboard instruments: a primary radar with a narrow swath, and a secondary sensor with a wider field of view that can only be used for lookahead. Similarly to SMICES [4], we defined a duty cycle of 20% so each radar measurement consumes 5% while the satellite battery recharges 1%

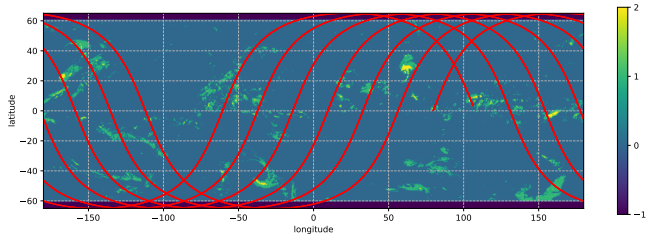

Fig. 1. Global data set and orbit with a 65 degree inclination. The simulation consists of 18,000 time steps spanning 10 hours. Three different classes of storm clouds were considered: no storm (0), lesser storm (1), and storm (2).

at each time step. General Mission Analysis Tool (GMAT) was used to simulate the orbital dynamics and to generate realistic satellite trajectories. We simulated a low Earth orbit with a 65 degree inclination (Figure 1), a 400 km altitude, an approximate period of 95 minutes, and an eccentricity of 0. The experiment consists of 18,000 time steps at 2 seconds per time step, spanning a total of 10 hours.

The previous parameters were chosen to emulate the Global Precipitation Measurement (GPM) mission [5]. GPM is a joint mission between NASA and JAXA to make frequent observations of Earth's precipitation. It works with a satellite constellation to provide full global coverage. GPM carries two instruments, here we focus on the Dual-frequency Precipitation Radar (DPR) which can measure precipitation characteristics in the atmospheric column in three dimensions and covers a 245 km swath. Additionally, we assumed it carries a lookahead sensor with a 680 km reach.

In order to identify storm clouds at a global scale we merged two different data products. The first one consists of precipitation estimates from the GPM Integrated Multi-satellitE Retrievals (IMERG) [6]. The second one consists of infrared brightness (IR) temperature data from the NOAA Climate Prediction Center/NCEP/NWS [7]. These two data products were aligned and resampled to a resolution of 4 km/pixel. IR data only covers latitudes within the $(-60°, 60°)$ range (Figure 1). Additionally, both data sources consist of half-hourly measurements from January 1st, 2020. Time interpolation was used in the simulation study to better capture the evolution of storms throughout time. These merged products allowed us to differentiate three different storm classes: no storm, lesser storm, and storm (Figure 1). Storms are much rarer than lesser storms, and so on. The corresponding precipitation and IR temperature thresholds for classification are shown in Table 1.

Table 1. Storm classification thresholds.

	Precipitation	IR Temperature
No storm	< 5 mm	> 240 K
Lesser storm	> 5 mm	> 240 K
Storm	> 5 mm	< 240 K

4. DYNAMIC TARGETING ALGORITHMS

In this work we compare six different algorithms (Figure 2). Four of them are dynamic targeting algorithms that are based on greedy heuristics and can be easily deployed onboard aircraft and spacecraft. The other two methods provide lower and upper bounds on performance.

4.1. Random

The random algorithm targets the pixel under nadir 20% of the time to ensure that it meets energy requirements. It is representative of most targeting methods on current Earth Science satellites. It is indifferent to the clouds it is flying over and will most likely miss many important storm clouds. It provides a lower bound on performance.

4.2. Greedy Nadir

The greedy nadir algorithm improves upon the random algorithm by controlling when the radar is turned on. It utilizes the system's current energy state and the storm cloud type under nadir to determine when the radar is turned on instead of making random decisions. This allows the system to save energy when there are no interesting clouds, and use the stored energy when there are storms.

4.3. Greedy Radar

The greedy radar algorithm expands its view along the path of the satellite to include the entirety of the radar's reachability. The state of charge determines which cloud types are able to be analyzed, and a simple greedy search inside of the radar's reachability finds the highest valued cloud with a tiebreaker going to the pixel that is closest to nadir.

4.4. Greedy Window

The greedy window algorithm expands its view using the lookahead sensor, meaning that it is able to account for future clouds along the radar's path. The algorithm first calculates how many clouds can be analyzed based on the current state of charge (SOC). It then counts the number of interesting storm clouds present within the knowledge window. The power is then allocated for all of the storm pixels, followed by the lesser storms, and then any leftover power is reserved as free. The highest valued pixel within the radar's view that has allocated power is imaged. The tiebreaker still goes to the pixel closest to nadir. The pixel under nadir is imaged if no storm clouds are within the radar's view, there is free power, and there is a sufficient SOC.

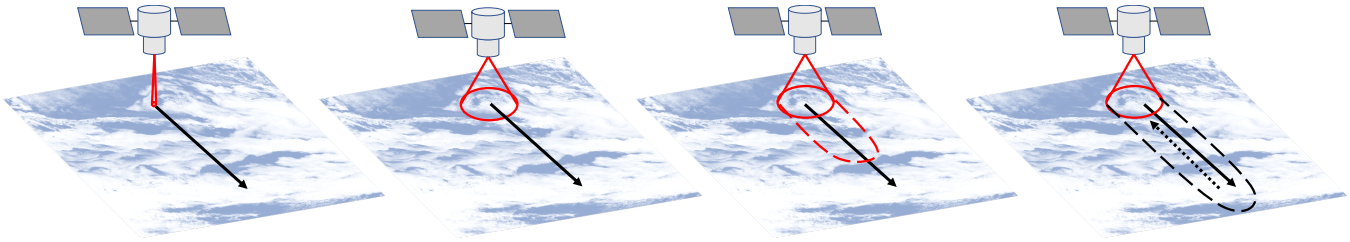

Fig. 2. Dynamic targeting algorithms for storm feature tracking. The random and greedy nadir algorithms are exclusively aimed at nadir (left). The greedy radar algorithm has a wider field of view and can collect samples off nadir, but is restricted by the radar's swath (center left). The greedy window and greedy path algorithms leverage a lookahead sensor with even more reach to better allocate resources for future measurements (center right). The dynamic programming approach has a full lookahead (assuming the path is finite) and achieves optimality via backward induction, however it cannot be deployed using realistic instrument and computational resources (right).

4.5. Greedy Path

Greedy path improves upon greedy window by ranking the priority of each storm and lesser storm pixel in the knowledge window. The algorithm begins by collecting the locations of all these pixels and calculating the available radar cycles based on the SOC. Once collected, the two pixel types are sorted independently by their lateral distance to nadir. This means that a newly scanned storm cloud pixel that will eventually cross nadir will have a higher priority than an off-nadir convection core pixel within the radar's view. The sorted list of lesser storm clouds is then concatenated to the end of the sorted list of storm cloud pixels to create a priority queue. Greedy path then assigns one radar cycle to the highest priority pixel and checks if it is within the radar's view. If it is viewable, the pixel is analyzed. Otherwise, it continues until the free cycles run out or the priority queue ends. If free cycles are left over after the end of the priority queue and the SOC is sufficient, the algorithm will analyze nadir.

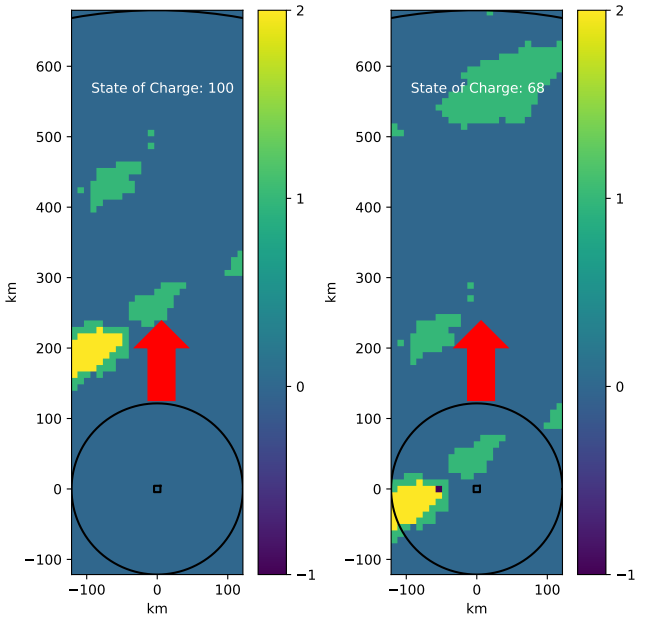

Fig. 3. Example of the greedy path algorithm. Left: It saves energy for valuable storm measurements in the near future, in this case within the lookahead sensor range. Right: A few time steps later, the algorithm uses the saved energy to track a storm that is now within the radar's reach.

4.6. Dynamic Programming

The dynamic programming (DP) algorithm is optimal and provides an upper bound on performance for the previous sampling methods. Its lookahead comprises the whole path to be traversed, which is assumed to be finite. The states are given by the location of the satellite and the SOC, while the actions consist of the pixels that are within the radar's reach. This algorithm uses backward induction to determine the optimal sequence of actions. The objective function is additive and the reward values for each storm type are as follows: no sample 0, no storm 1, lesser storm 1×10^4, and storm 1×10^8. These values virtually eliminate tradeoffs among different cloud types. Finally, the tiebreaker goes to pixels closest to nadir. Unfortunately, this algorithm cannot be deployed in most cases onboard aircraft or spacecraft for the following reasons. First, it is computationally expensive and planning requires minutes or hours depending on the total path length; second, a lookahead sensor with such range is unrealistic. However, this algorithm is valuable for evaluation and comparison purposes.

5. RESULTS

Overall we observe that DT methods are good at choosing when to save energy and when to collect measurements (Figure 3). Results indicate that DT delivers a significant increase in performance (Table 2). The baseline random algorithm is always outperformed and tends to gather too much non-storm data because it does not use any auxiliary information. The

Table 2. DT algorithms' performance as percentages of analyzed clouds per storm category. Random and DP provide lower and upper bounds on performance, respectively.

Algorithm	Off	No Storm	Lesser Storm	Storm
Random	80.03%	18.21%	1.69%	0.07%
G. Nadir	79.53%	15.87%	4.42%	0.18%
G. Radar	76.69%	7.81%	14.58%	0.92%
G. Window	79.75%	6.92%	11.39%	1.93%
G. Path	79.75%	6.92%	11.12%	2.21%
DP	79.69%	6.28%	11.40%	2.63%

greedy nadir approach has a slightly better performance, but it is still very constrained. Greedy radar does a much better job since it can sample from many more pixels, however it samples too many lesser storms. Greedy window and greedy path perform even better because they exploit the information from the lookahead sensor to save energy more effectively. DP, as expected, outperforms the rest as it is omniscient and optimal. Nonetheless, despite substantially more limited lookaheads (250 km against 40,075 km), most DT algorithms have a performance that is decently close to the optimum.

6. CONCLUSIONS AND FUTURE WORK

This work discusses DT as a powerful approach that leverages lookahead sensor data to optimize the utilization of a primary sensor, commonly subject to operation constraints, and thus improve science return. We describe several DT algorithms and test them via a realistic simulation study that involves storm feature tracking. The experimental results indicate that DT is a very promising approach. When comparing the best performing algorithm, greedy path, against the baseline random algorithm, significantly more storm clouds are sampled while respecting energy constraints. Furthermore, the DT algorithms tend to have a competitive performance when compared to our dynamic programming method.

Future work will keep improving the realism of our simulation study; for instance, we plan to capture more physical constraints such as off-nadir measurements with deteriorating quality. Further research will continue to investigate the advantages of DT using other cloud and storm data sets. Finally, working closely with leading scientists, we will refine use cases and quantify performance improvement for other application domains such as tracking volcanic targets.

7. ACKNOWLEDGEMENTS

The research was carried out at the Jet Propulsion Laboratory, California Institute of Technology, under a contract with the National Aeronautics and Space Administration (NASA) (80NM0018D0004). This work was supported by the Earth Science and Technology Office (ESTO), NASA.

8. REFERENCES

[1] D. R. Thompson et al., "Rapid spectral cloud screening onboard aircraft and spacecraft," *IEEE Transactions on Geoscience and Remote Sensing*, vol. 52, no. 11, pp. 6779–6792, 2014.

[2] H. Suto et al., "Thermal and near-infrared sensor for carbon observation Fourier transform spectrometer-2 (TANSO-FTS-2) on the Greenhouse gases Observing SATellite-2 (GOSAT-2) during its first year in orbit," *Atmospheric Measurements Techniques*, vol. 14, 2021.

[3] Z. Hasnain et al., "Agile Spacecraft Imaging Algorithm Comparison for Earth Science," in *International Workshop on Planning and Scheduling for Space (IWPSS)*, 2021.

[4] J. Swope et al., "Using Intelligent Targeting to increase the science return of a Smart Ice Storm Hunting Radar," in *International Workshop on Planning and Scheduling for Space (IWPSS)*, 2021.

[5] Huffman, G. and others, "Integrated Multi-satellitE Retrievals for GPM (IMERG), version 4.4," `ftp://arthurhou.pps.eosdis.nasa.gov/gpmdata/`, 2014, NASA's Precipitation Processing Center. Accessed: 2017-11-01.

[6] Huffman, G.J. and others, "GPM IMERG Final Precipitation L3 Half Hourly 0.1 degree x 0.1 degree V06," `https://disc.gsfc.nasa.gov/datasets/GPM_3IMERGHH_06/summary`, 2019, Greenbelt, MD, Goddard Earth Sciences Data and Information Services Center (GES DISC). Accessed: 2017-11-01.

[7] Janowiak, J. and Joyce, B. and Xie, P., "NCEP/CPC L3 Half Hourly 4km Global (60S - 60N) Merged IR V1," `https://doi.org/10.5067/P4HZB9N27EKU`, 2019, Greenbelt, MD, Goddard Earth Sciences Data and Information Services Center (GES DISC). Accessed: 2017-11-01.